

## A solitary wave model for sedimentation in colloidal suspensions

This article has been downloaded from IOPscience. Please scroll down to see the full text article.

1987 J. Phys. A: Math. Gen. 20 305

(<http://iopscience.iop.org/0305-4470/20/2/016>)

View [the table of contents for this issue](#), or go to the [journal homepage](#) for more

Download details:

IP Address: 129.252.86.83

The article was downloaded on 01/06/2010 at 05:20

Please note that [terms and conditions apply](#).

# A solitary wave model for sedimentation in colloidal suspensions

G C Barker and M J Grimson

AFRC Food Research Institute, Colney Lane, Norwich NR4 7UA, UK

Received 4 February 1986

**Abstract.** Burgers' equation is used to model sedimentation of colloidal suspensions in terms of solitary waves. The importance of diffusive terms is highlighted. Analytic expressions are given for the distribution of dispersed material and the wavefront velocities are calculated as functions of time. An explanation of observed sedimentation behaviour is provided along with a discussion of the important features of real sedimenting systems.

## 1. Introduction

We shall present some simple expressions for the variation of concentration profile with time in a model colloidal dispersion undergoing sedimentation. The results, which are exact within the model and which can be expressed in terms of a small number of easily interpreted parameters, provide a representation of sedimentation phenomena which facilitates immediate comparison with experiments. There are many important examples of these phenomena, in which a two-phase material is separated under the action of an external field (e.g. blood purification, food emulsion stability, oil recovery) but here we concentrate on general expressions rather than details of particular systems.

The simplest observations of sedimentation show, for an initially homogeneous sample, the formation and propagation of a meniscus. Occasionally two menisci are observed moving towards each other and in special circumstances there may be several (Siano 1979). For a large part of the experiment the interface(s) travel parallel or antiparallel to the external field and apparently without change of form. Finally there is a single interface at rest separating essentially pure solvent from a concentrated sediment which has an amorphous structure. These facts suggest a one-dimensional solitary wave formulation of sedimentation which is previously unknown to the authors. The pertinent features will be seen to be included in a simple non-linear partial differential equation (Burgers' equation) which is derived in § 2.

The detailed dynamics of colloiddally sized objects supported in viscous fluid and placed in an external field have received extensive theoretical study. However the microscopic framework for evaluating the mobility tensors and settling velocities (Batchelor (1976, 1982), although recently extended to include size polydispersity (Batchelor 1982), repulsive interparticle interactions (Dickinson 1980) and many-body hydrodynamics (Mazur 1985)) is sufficiently complex to limit all results to low-order series expansions in the volume fraction  $\phi$  of the dispersed phase and therefore restrict applications to dilute systems.

We may identify several aspects of real sedimenting colloids which hinder comparisons with rigorous theoretical treatments.

(i) Aggregation processes, both reversible and irreversible (coagulation), lead to the formation of time dependent cluster and size distributions even for inherently monodisperse systems. Brownian dynamics simulations of model colloids show that the underlying association and disassociation rates, and therefore the induced polydispersity and the complex flows associated with the porous aggregates, are strongly influenced by the details of the interparticle interactions including the attractive portions. It is precisely these details which remain unknown in the majority of cases and which cannot be incorporated in the Batchelor formalism therefore limiting the range of fully self-contained microscopic calculations.

(ii) The ability of many colloidal droplets to deform introduces (a) significant changes in the pair distribution of the drops (Dickinson 1984) and therefore changes in the effect of interparticle forces and (b) unknown modifications of the direct and indirect (hydrodynamic) interparticle interactions themselves. The microscopic framework depends on rigid particles.

(iii) The two-component picture is rarely realised in practice. Often the continuous phase contains a dissolved third component (polymer, electrolyte, polysaccharide) and may be inhomogeneous; alternatively surface active material may be present or the dispersed objects may be complex (irregular shapes, capsular, etc).

Many of the unresolved problems will be absorbed by choosing a continuous field formulation with phenomenological dynamics. Within this scheme we shall build a model which allows qualitative comparison with the wealth of experimental results but remains sufficiently transparent to provide a reference for discussion of the important points above. Thus we consider monodisperse, non-aggregating particles, sedimenting in an external field which varies in only one spatial direction  $y$ , and include all the details of dynamics and interactions into a single function  $J(\phi, \partial\phi/\partial y)$  representing the flux of particles in a particular local environment. Here  $\phi = \phi(y, t)$  is a function of space and time and is the continuous field variable for our solitary wave picture. In general  $J$  may have a complicated dependence on particle volume fraction but for simplicity we make a separation

$$J(\phi, \partial\phi/\partial y) = \phi v(\phi) - \delta \partial\phi/\partial y \quad (1.1)$$

where  $v(\phi)$  is a single-particle velocity function (which we expect to increase towards the Stokes value for decreasing  $\phi$ ) and  $\delta$  is a positive constant. Further restrictions on (1.1) will be made in the following section: we consider only small values of  $\delta$  and the simplest possible form for  $v(\phi)$ . We have refrained from pursuing the computational methods necessary for more complex velocity functions, thereby retaining analytic results. The extension is straightforward.

The model presented will give the variation of volume fraction  $\phi(y, t)$  of a plug of dispersed phase material with known initial distribution located in an infinite tube between close packed sediment and pure solvent. When  $\delta \ll 1$  this can be used as an approximation to the behaviour observed in a finite tube where strictly the boundaries are fluxless.

## 2. Burgers' equation

Our approach is based on the classical theory of sedimentation due to Kynch (1952) which assumes that the settling process is determined by local conditions and can therefore be formulated as a continuity equation for the dispersed phase. This has

recently been used by Anselmet *et al* (1985) to interpret experimental sedimentation data. We include an extra small term in the particle flux (1.1) proportional to the concentration gradient and thereby remove the sharp discontinuities present in Kynch solutions. At the same time we choose a linear velocity function

$$v(\phi) = u_0(1 - \phi/\phi_m) \quad (2.1)$$

where  $u_0$  and  $\phi_m$  are constants;  $u_0$  is interpreted as the settling velocity of a single particle in unbounded fluid (Stokes' velocity) and  $\phi_m$  represents a maximum packing condition. Although more complex functions have been suggested for  $v(\phi)$  (Buscall *et al* 1982), equation (2.1) may always be regarded as a first approximation and contains the essential physics. In addition it allows us to circumvent the cumbersome method of characteristics or numerical integration and obtain analytic solutions.

In dimensionless form we may now write the continuity equation for the dispersed phase material as

$$\partial c/\partial \theta - (1 - 2c)\partial c/\partial y - \varepsilon \partial^2 c/\partial y^2 = 0 \quad (2.2)$$

where the concentration  $c(y, \theta)$  represents the volume fraction expressed in units of  $\phi_m$ . All lengths are scaled by the length  $L$  of the inserted plug of non-equilibrium material (origin of  $y$  is taken as the base of the inserted plug and the external field points along the negative  $y$  axis) and  $\theta$  is time scaled by  $|u_0|/L$ . The small parameter in dimensionless form is  $\varepsilon = |\delta/u_0L|$ . Equation (2.2) is Burgers' equation. A particular transformation due to Hopf and Cole linearises (2.2) and leads to a formal solution (Witham 1974)

$$c(y, \theta) = \int_{-\infty}^x c(z, 0) \exp(f(y, \theta, z)) dz \left( \int_{-\infty}^x \exp(f(y, \theta, z)) dz \right)^{-1} \quad (2.3)$$

where

$$f(y, \theta, z) = -(y - z + \theta)^2/4\varepsilon\theta + (1/\varepsilon) \int_z^x c(z', 0) dz'. \quad (2.4)$$

For the model outlined in § 1 we have initial concentration distribution

$$\begin{aligned} c(y, 0) &= 1 & y < 0 \\ &= c(y) & 0 \leq y \leq 1 \\ &= 0 & y > 1 \end{aligned}$$

and the exterior portions of the integrals (2.3) yield straightforward results:

$$\begin{aligned} \int_{-\infty}^0 \exp(f(y, \theta, z)) dz &= \int_{-\infty}^0 c(z, 0) \exp(f(y, \theta, z)) dz \\ &= (\pi\varepsilon\theta)^{1/2} \exp((c_0 - y)/\varepsilon) \operatorname{erfc}[(y - \theta)/(4\varepsilon\theta)^{1/2}] \end{aligned} \quad (2.5)$$

$$\int_1^{\infty} \exp(f(y, \theta, z)) dz = (\pi\varepsilon\theta)^{1/2} \operatorname{erfc}[(1 - y - \theta)/(4\varepsilon\theta)^{1/2}] \quad (2.6)$$

where  $c_0 = \int_0^1 c(y) dy$  is the initial non-equilibrium material. Complete evaluation of  $c(y, \theta)$  therefore requires

$$I_n = \int_0^1 c^n(z) \exp(f(y, \theta, z)) dz. \quad (2.7)$$

In a realistic example the initial distribution has discontinuities at  $y = 0, 1$  and these result in the dominant features or 'steps' in the evolving profile. We define their positions by a maximum gradient or  $\partial^2 c / \partial y^2 = 0$  which is consistent with the contrast determinations of this position commonly employed in the experimental work. Differentiating (2.3) twice we obtain

$$0 = c^3 + ac + b \quad (2.8)$$

where

$$a = -\frac{3}{2} \int_{-x}^x (c^2(z, 0) - \varepsilon \partial c(z, 0) / \partial z) \exp(f(y, \theta, z)) dz \left( \int_{-x}^x \exp(f(y, \theta, z)) dz \right)^{-1} \quad (2.9)$$

$$b = \frac{1}{2} \int_{-x}^x (c^3(z, 0) - 3\varepsilon c(z, 0) \partial c(z, 0) / \partial z + \varepsilon^2 \partial^2 c(z, 0) / \partial z^2) \exp(f(y, \theta, z)) dz \left( \int_{-x}^x \exp(f(y, \theta, z)) dz \right)^{-1}. \quad (2.10)$$

Equation (2.8) is an implicit relation between step position and time. In all but the simplest cases a numerical solution is required.

The origin of the diffusive flux in (1.1) has been discussed in detail by Batchelor (1976). The classical theory of Brownian motion extended to non-equilibrium systems, and therefore including hydrodynamic as well as direct particle-particle interactions, leads to a generalised force which accounts for diffusive transport in inhomogeneous systems. Since it is apparent that a sedimenting dispersion contains highly inhomogeneous regions the third term in (2.2) cannot be neglected. However simple estimates of the size of the parameter,  $\sim kT/Lmg$  ( $m$  is particle mass,  $T$  temperature and  $k$  Boltzmann's constant), are smaller than required by comparisons with experimental profiles. The non-ideal features of sedimentation listed above may contribute to this discrepancy (for example, by causing smaller particles to congregate at the interface). However there are two significant features associated with the fact that the important particles in the determination of  $\varepsilon$  are those located around sharp steps in concentration. First, Pusey and Tough (1982) have pointed out that Batchelor's approach is relevant for timescales which are much bigger than velocity fluctuation times caused by fluid particle impacts yet much smaller than a 'structural relaxation' time. In the vicinity of the interface the statistical properties of the particle velocities may be a consequence of spatial configuration so that collective processes on larger timescales could be relevant. Second, the particulate environment changes very rapidly as we move through the interface causing relevant length scales to be shorter. This may invalidate the continuum approximation for the suspending fluid and necessitate a full multicomponent microscopic treatment surrounding the meniscus.

In the following section  $\varepsilon$  is used as the only variable parameter. Quantitative interpretation requires detailed specification of the particular systems involved.

### 3. Results and discussion

The majority of experimental investigations begin with a uniform distribution of

dispersed material. In this case  $c(y) = c_0$  and integrals in (2.3) are completed by

$$I_0 = (\pi\epsilon\theta)^{1/2} \exp\{c_0[1 - y - \theta(1 - c_0)/\epsilon]\} \left\{ \operatorname{erfc}[(2\theta c_0 - y - \theta)/(4\epsilon\theta)^{1/2}] - \operatorname{erfc}[(1 - y - \theta + 2\theta c_0)/(4\epsilon\theta)^{1/2}] \right\} \quad (3.1)$$

and

$$I_1 = c_0 I_0. \quad (3.2)$$

Combining equations (3.1) and (3.2) with (2.5) and (2.6) we may compute the full concentration profiles. Figure 1 shows the evolution of an initially flat or constant profile with  $c_0 = 0.3$ ,  $\epsilon = 0.015$  from small  $\theta$  until an equilibrium is achieved (broken curve). The curves show two ‘tanh-like’ solitary waves which propagate towards each other from initial positions  $y = 0, 1$ . These features are localised and therefore the initial profile is undisturbed until approached by one of the waves. Finally the two fronts coalesce and ‘stiffen up’ into an equilibrium profile around  $y = c_0$ . In figure 1 two steps are discernable for  $\theta \leq 1$ . At larger values of  $\epsilon$  both steps are more diffuse. Also a larger disparity between the sizes of the two steps reduces the definition of the smaller. In some cases (e.g.  $c_0 = 0.2$ ,  $\epsilon = 0.04$ ) these factors combine to make a single shock or wavefront the dominant feature.

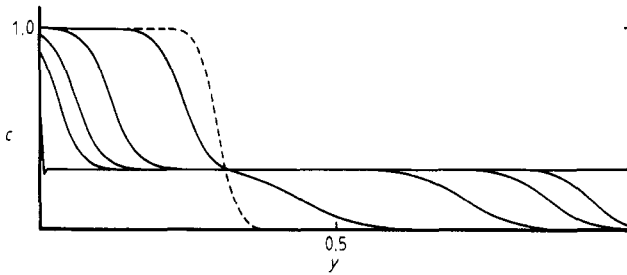


**Figure 1.** Distribution of dispersed material at  $\theta = 0.0001, 0.1, 0.2, 0.4, 0.8$  and  $8.0$  (broken curve). The initial distribution is uniform with  $c_0 = 0.3$ ,  $\epsilon = 0.015$ . The external field is directed along the negative  $y$  axis.

For a uniform initial distribution we may write equation (2.8) in a particularly simple form. All the derivatives in (2.9) and (2.10) are zero and we write contributions to the denominator of (2.3) from (2.5), (3.1) and (2.6) as  $P$ ,  $Q$  and  $R$  respectively. Positions of the wavefronts are now given by

$$0 = (c_0 - 1)^3 PQ(P - Q) + PR(R - P) + c_0^3 QR(R - Q) + (2c_0^3 - 3c_0^2 - 3c_0 + 2)PQR. \quad (3.3)$$

If  $R$  is insignificant ( $\theta \ll 1$ ,  $y \approx 0$ ) we have  $P = Q$  and from (3.1) and (2.5) the solution  $y = c_0\theta$ . Similarly for  $\theta \ll 1$ ,  $y \approx 1$  we obtain  $y = 1 - (1 - c_0)\theta$ . Thus for small  $\theta$  the two shocks have constant velocities  $c_0|u_0|$  and  $-(1 - c_0)|u_0|$ . For larger times the simple form of (3.3) allows us to follow the roots numerically. Figure 2 shows the variation of the velocity of the major shock (in units of  $|u_0|$ ) with  $\theta$  for  $\epsilon = 0.03$  and  $c_0 = 0.1-0.4$ . The second smaller shock gathers speed towards  $y = c_0$  but disappears as the waves coalesce. Figure 2 clearly shows a change of behaviour as  $c_0$  is increased. The curves representing higher values of initial concentration show a region of acceleration (which is enhanced by higher values of  $\epsilon$ ) prior to decelerating to equilibrium. This effect is associated with the change of value of concentration for which our shock condition holds. Using (2.2) we can express the full derivative as

$$dy/d\theta = (2c - 1) + (\partial y/\partial c)(\partial c/\partial \theta) + \epsilon(\partial y/\partial c)(\partial^2 c/\partial y^2). \quad (3.4)$$

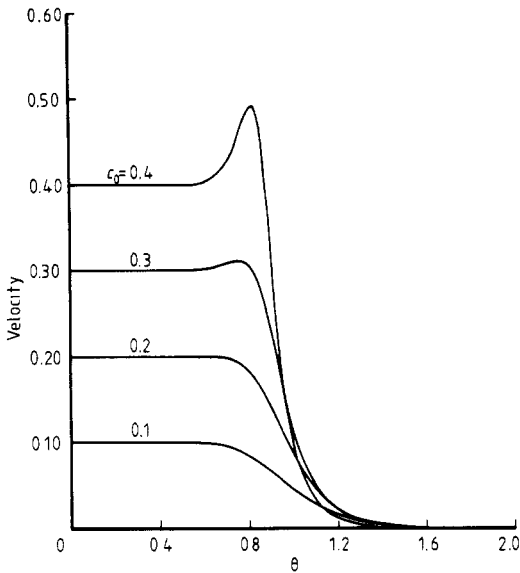


**Figure 2.** Major shock velocity (units of  $|u_0|$ ) as a function of  $\theta$  for  $c_0 = 0.1, 0.2, 0.3, 0.4$  and  $\varepsilon = 0.03$ . The initial material distribution is uniform.

Initially the waves propagate without change of form and the first term alone determines the velocity of the fronts but as the waves collide the second term is relevant. The major shock transfers from  $c = (1 + c_0)/2$  ( $\theta \ll 1$ ) to  $c = \frac{1}{2}$  at equilibrium and hence it is for higher initial concentrations that the  $\partial c / \partial \theta$  term is most important.

Recently Anselmet *et al* (1985) have presented measurements of the upper meniscus position in a sedimenting suspension of monodisperse spheres and identified two regimes, namely initial concentrations above or below the concentration of maximum flux  $c_M$ , which show qualitatively different behaviours. For  $c_0 < c_M$  planes of constant concentration  $c_0/2$  show a single sedimentation velocity followed by an abrupt halt whereas for  $c_0 > c_M$  there is a prolonged continuous deceleration of the interface. The interpretation of Anselmet *et al*, using the theory of Kynch (1952) (i.e. no diffusive terms) with a non-linear velocity function, involves a constant size but stiffening discontinuity for  $c_0 < c_M$  and a growing discontinuity for  $c_0 > c_M$ . The experimental results are unable to confirm these features.

In contrast the solutions (2.3) propagate without change of form for long periods. For planes of constant concentration the second term in (3.4) is zero but velocity changes can result from the third term (also zero in the Anselmet *et al* consideration) with increasing importance for larger  $c_0$ . This term is also sensitive to small gradients in the initial distribution leading to a continuously variable meniscus velocity. Figure 3 gives the speed of planes  $c = c_0/2$  for  $\varepsilon = 0.015$ ,  $c_0 = 0.05, 0.65$  (note for our linear function  $c_M = 0.5$ ) and an initial gradient  $\Delta c / c_0 = 0.05$ . There is a period of much larger deceleration for  $c_0 = 0.05$  and a steadily decreasing velocity for  $c_0 = 0.65$  in qualitative agreement with the observations of Anselmet *et al*. With no initial gradient the effects at large values of  $c_0$  are less pronounced.

Figure 3 also shows an enhanced meniscus velocity at very small times. This is a result of relaxation from the initial discontinuous distribution into a steady profile. Generally planes of constant concentration at non-symmetric points in the profile (i.e.

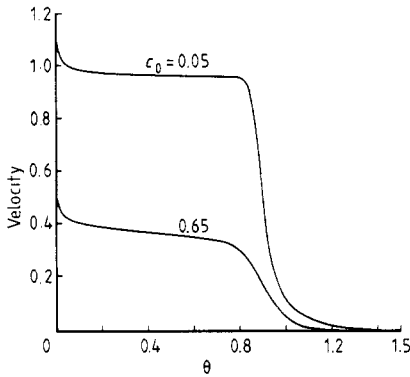


**Figure 3.** Velocity of plane  $c = c_0/2$  (units of  $|u_0|$ ) as a function of  $\theta$  for  $c_0 = 0.05, 0.65$  and  $\epsilon = 0.015$ . The initial material distribution has a gradient  $\Delta c/c_0 = 0.05$  in the direction of the external field.

planes other than  $(1 + c_0)/2$  and  $c_0/2$  in initially flat profiles) have an initial motion relative to the symmetric point which contributes to the velocity through the third term in (3.4). In particular when the initial profile has a slope the symmetry point shifts as the meniscus moves and therefore plane  $c = c_0/2$  also exhibits this behaviour. Transient effects in which part of the meniscus travel faster than the Stokes' velocity of the constituent particles are possible for small concentration steps. By adopting the contrast definition we can isolate the meniscus velocity from relative motion in the interface.

Solutions of equation (2.2) are not restricted to the uniform initial distributions discussed above. Analytic solutions can be obtained for any piecewise linear or quadratic  $c(y)$ . As an example consider the evolution of an initial ramped sawtooth distribution of very low overall concentration,  $c_0 = 0.01$ , shown in figure 4. A staircase pattern persists for a considerable period and propagates, lower steps most rapidly, into the small sediment. This layered sedimentation behaviour has been observed in dilute suspensions of polystyrene spheres by Siano (1979). The initial formation may result from either local fluctuations of concentration which are enhanced and tilted by the gradient set up in an initial sedimentation process or from a phase separation phenomenon recently discussed by Hagan and Cohen (1985).

Using a two-fluid model and a variational derivation of the equations of motion Hill *et al* (1980) were able to obtain a representation of erythrocyte sedimentation in human whole blood which naturally included diffusive terms. The particle dynamics were included through an empirical drag coefficient as a function of  $\phi$ . The numerical results are in reasonable agreement both with experimental concentration profiles

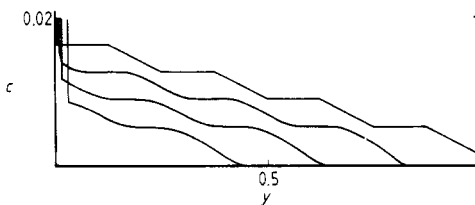


**Figure 4.** Distribution of dispersed material at  $\theta = 0.0001, 0.2, 0.4$  and  $1.5$ . The initial material distribution is a ramped sawtooth with  $c_0 = 0.01, \epsilon = 0.001$ . The external field is directed along the negative  $y$  axis.



(Whelan *et al* 1971) and with our analytic treatment confirming the importance of dissipative effects.

Although our results are for the simplest possible non-linear dissipative system they have the capacity to successfully represent a wide variety of sedimentation results and also form a prototype for extensions to numerical work. In this respect the precise forms of  $v(\phi)$  and any functional dependence of  $\varepsilon$  do not present serious problems. However, any discussions of wall effects on sedimentation (Beenaker and Mazur 1985) are incompatible with our one-dimensional approach, the inclusion of polydispersity, in any form, is severely hampered by the non-linearity of Burgers' equation, and our approach via a continuity equation prevents consideration of inertial effects.

Clearly our results support continued improvement of non-intrusive scanning of full concentration profiles. They also show that more rigorous definition and resolution in optical determinations of meniscus positions, and therefore velocities, are justified. Finally our results indicate that a detailed specification of initial conditions is required for quantitative discussion of sedimentation experiments.

## References

- Anselmet M C, Anthore R, Auvray X, Petipas C and Blanc R 1985 *C.R. Acad. Sci., Paris* **300** 993  
 Batchelor G K 1976 *J. Fluid Mech.* **74** 1  
 ——— 1982 *J. Fluid Mech.* **119** 379  
 Beenaker C W J and Mazur P 1985 *Phys. Fluids* **28** 3203  
 Buscall R, Goodwin J W, Ottewill R H and Tadros Th F 1982 *J. Colloid Interface Sci.* **85** 78  
 Dickinson E 1980 *J. Colloid. Interface Sci.* **73** 578  
 ——— 1984 *Phys. Rev. Lett.* **53** 728  
 Hagan P S and Cohen D S 1985 *Physica* **17D** 54  
 Hill C D, Bedford A and Drumheller D S 1980 *J. Appl. Mech.* **47** 261  
 Kynch G J 1952 *Trans. Faraday Soc.* **48** 166  
 Mazur P 1985 *Can. J. Phys.* **63** 24  
 Pusey P N and Tough R J A 1982 *J. Phys. A: Math. Gen.* **15** 1291  
 Siano D B 1979 *J. Colloid Interface Sci.* **68** 111  
 Whelan J A, Huang C R and Copley A L 1971 *Biorheology* **7** 205  
 Witham G B 1974 *Linear and nonlinear waves* (New York: Wiley)